Electronic Supplementary Material (ESI) for Nanoscale.
This journal is © The Royal Society of Chemistry 2019

ELECTRONIC SUPPLEMENTARY INFORMATION (ESI)

Ti_3C_2 MXene quantum dots-encapsulated liposome for photothermal immunoassay using a portable near-infrared imaging camera on smartphone

Guoneng Cai,[a] Zhenzhong Yu,[a] Ping Tong[b,*] and Dianping Tang[a,*]

[a]Key Laboratory for Analytical Science of Food Safety and Biology (MOE & Fujian Province), State Key Laboratory of Photocatalysis on Energy and Environment, Department of Chemistry, Fuzhou University, Fuzhou 350108, China

[b]Testing Center, Fuzhou University, Fuzhou 350108, China

CORRESPONDING AUTHOR INFORMATION

Phone: +86-591-2286 6125; fax: +86-591-2286 6135; e-mails: tping@fzu.edu.cn (P.T.) & dianping.tang@fzu.edu.cn (D.T.)

TABLE OF CONTENTS

EXPERIMENTAL SECTION

Material and Chemical. Powders of aluminum titanium carbide (Ti_2AlC_3, 98%, 200 mesh) were purchased from Forsman Technology Co., Ltd. (Beijing China). Hydrofluoric acid (HF, 48%), chloroform, $NaH_2PO_4 \cdot 2H_2O$, $Na_2HPO_4 \cdot 12H_2O$ and NaCl were acquired from Sinopharm Chem. Re. Co., Ltd. (Shanghai, China). Tetramethylammonium hydroxid (TMAOH, 25 wt %), 1,2-dipalmitoyl-sn-glycero-3-phosphatidylethanolamine (DPPE), 1,2-dipalmitoyl-sn-glycero-3-phospho choline (DPPC) and cholesterol were achieved from Aladdin (Shanghai, China). Prostate-specific antigen (PSA), monoclonal anti-PSA-021 capture antibody (mAb1), monoclonal anti-PSA-173 detection antibody (mAb2), carcinoembryonic antigen (CEA), alpha-fetoprotein (AFP), immunoglobulin M (IgM), immunoglobulin A (IgA), and dialysis bag (MW cutoff 100 KDa) were gotten from Sangon Biotech. Co., Ltd. (Shanghai, China). Triton X-100, bovine serum albumin (BSA), immunoglobulin G (IgG), thrombin (Thb) and bovine serum were obtained from Dingguo Biotech. Co., Ltd. (Beijing, China). All chemical reagents in this study were of analytical grade and were used without further purification. Millipore Milli-Q water (18.2 MΩ·cm) was used throughout the experiment.

Apparatus. High-resolution transmission electron microscopy (HRTEM) was carried out on FEI Talos F200S G2 at 200 KV accelerating voltage (Thermo Fisher Scientific Co., Ltd). Field scanning electron Microscopy (FSEM) was executed on Nova NanoSEM 230 (FEI Czech Republc S.R.O. Co., Ltd). Atomic force microscopy (AFM) was implemented on Nano Scope II 5500AFM/SPM (Agilent Technologies Co., Ltd., Santa Clara, CA, USA). X-Ray diffraction (XRD) patterns were characterized by BRUKER D2 PHASER diffractometer equipped with Cu Kα irradiation (λ = 1.54184 Å) and worked at 10 mA and 30 kV. X-ray photoelectron spectra (XPS) was obtained from ESCALAB 250 (Thermo-VG Scientific Co., Ltd). UV-vis absorption spectra was recorded on an Infinite M200 Pro of TECAN GENIOS with QS-grade quartz cuvettes at room temperature. Fourier transform Infrared (FT-IR) spectra was registered on a Nicolet (Thermo Scientific Co., Ltd). Fluorescence emission spectra and excitation spectra were obtained on F-4600 Flspectorophotomet (Hitachi, Tokyo, Japan). Dynamic light scattering (DLS) and ζ- potential measurement were conducted from Zetasizer Nano-ZS90 (Malvern Panalytical

Co., Ltd). The 808-nm near-infrared light source was purchased from Shenzhen Infrared Laser Techn. Co., Ltd (Shenzhen, China). The temperature curve was measured by VICTOR 86 digital thermometer (Xi'an Beicheng Electronic Co., Ltd, China). The near-infrared images were taken by FLIR near-infrared imaging camera of FLIRSystems Inc. The portable measurement fixture was produced by 3D printer (Form 2) of Formlabs Co., Ltd.

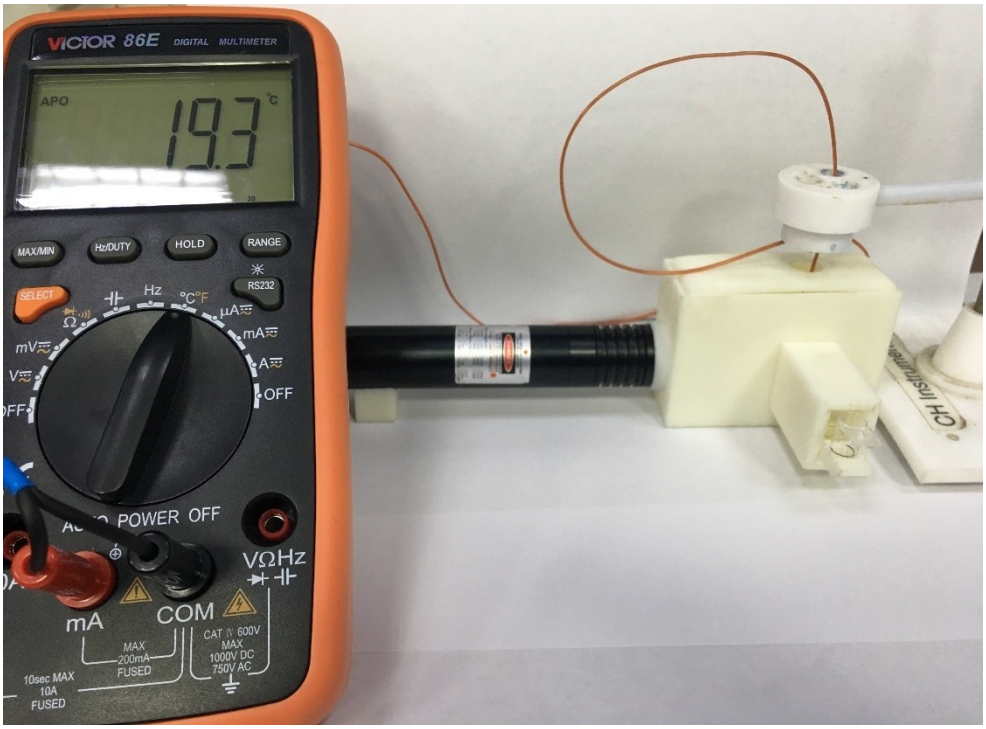

Scheme S1 Illustration of photothermal immunoassay device on a thermometer.

PARTIAL RESULTS AND DISCUSSION

Calculation of Photothermal Conversion Efficiency. Photothermal conversion efficiency of Ti_3C_2 QDs was calculated according to the previous reports.[1,2] Detailed calculation was given as follows. The total energy balance for the whole system is

$$\sum_i m_i C_{p,i} \frac{dT}{dt} = Q_{QDs} + Q_{Dis} - Q_{Surr} \quad (1)$$

Where: m and C_p are the mass and heat capacity, respectively. T refers to the solution temperature. Q_{QDs} is the photothermal energy input of Ti_3C_2 QDs. Q_{Dis} is the photothermal energy input of solvent and water and container. Q_{Surr} is the heat energy conducted away from the system to the surrounding.

Q_{QDs} expresses heat dissipated by electron-phonon relaxation of the plasmon on the surface of Ti_3C_2 QDs under the 808 nm (λ) laser irradiation.

$$Q_{QDs} = I(1-10^{-A_\lambda})\eta \qquad (2)$$

Where: I is the incident power of the NIR laser (mW), A_λ is the absorbance of the Ti_3C_2 QDs at the NIR laser wavelength (λ) of 808 nm in aqueous solution, and η is the photothermal conversion efficiency of Ti_3C_2 QDs from the incident NIR laser energy to thermal energy. Q_{Surr} represents a temperature-dependent parameter, which is linear with thermal energy lost

$$Q_{Surr} = hS(T - T_{Surr}) \qquad (3)$$

Where: h is the heat transfer coefficient, S is the surface area of the container, T is temperature of system surface, and T_{Surr} is the surrounding temperature, respectively.

Q_{Dis} is the heat associated with the light absorbed by solvent water and quartz cuvette sample cell. Once the NIR laser power is defined, the heat input (Q_{QDs} + Q_{Dis}) will be finite, the heat input is equal to the heat output at the maximum steady-statue temperature, so the equation could be:

$$Q_{QDs} + Q_{Dis} = Q_{Surr\text{-}Max} = hS(T_{Max} - T_{Surr}) \qquad (4)$$

T_{Max} is the equilibrium temperature, standing for no heat conduction away from the system surface by air. Besides, Q_{Dis} represents the heat dissipated from the photo absorption of the quartz cuvette sample cell itself, and it was measured independently to be using a sample cell containing pure water without Ti_3C_2 QDs.

In order to obtain photothermal conversion efficiency (η), substituting eq 3 for Q_{QDs} into eq 5 and rearranging, η can be expressed as following:

$$\eta = \frac{hS(T_{Max} - T_{Surr}) - Q_{Dis}}{I(1-10^{-A_\lambda})} \qquad (5)$$

Therefore, in this equation, only the hS is unknown for the calculation of η. In order to obtain hS, we introduce a Θ defined as dimensionless driving force temperature, and a τ_s representing a time constant of sample system,

$$\theta = \frac{T - T_{Surr}}{T_{Max} - T_{Surr}} \qquad (6)$$

$$\tau_s = \frac{\sum_i m_i C_{p,i}}{hS} \qquad (7)$$

which substituted into eq (2) and rearranged to yield

$$\frac{d\theta}{dt} = \frac{1}{\tau_s}\left[\frac{Q_{QDs} + Q_{Dis}}{hS(T_{Max} - T_{Surr})} - \theta\right] \quad (8)$$

When the Ti_3C_2 QDs was cooling, the laser radiation ceases and $Q_{QDs} + Q_{Dis} = 0$ eq (8) could be expressed to:

$$dt = -\tau_s \frac{d\theta}{\theta} \quad (9)$$

and the final expression after integrating

$$t = -\tau_s In\theta \quad (10)$$

All the parameters using in the equation are as follows. For the measurement of Ti_3C_2 QDs, the T_{Max} was 37.7 °C and the T_{Surr} was 25.1 °C. Through linear fitting, τ_s was about 285.74 s. The temperature change (T_{Max} - T_{Surr}) was 12.6 °C. Compared with m_{H_2O}, the m_{QDs} (2.0 × 10^{-9} kg) was too little so it could be neglected. Therefore, the $m_iC_{p,i}$ was calculated by m_{H_2O} (1.0 × 10^{-3} kg) and $C_{p,i}$ (4.2 J/g·°C). According to the results mentioned before, the *hS* was deduced to be 14.69 mW/°C. In addition, the laser power *I* was 1000 mW where the area of light spot was 1.0 cm^2, and the absorbance of the Ti_3C_2 at 808 nm (A_{808}) was 0.2057. Q_{Dis} was measured independently to be 29.38 mW. Thus, the photothermal conversion efficiency (η') of Ti_3C_2 QDs could be calculated by substituting according values of each parameters to eq (6) that was 41.27%. The photothermal conversion efficiency of Ti_3C_2 nanosheets (η') was calculate similarly, where the T_{Max} was 40.2 °C and T_{Surr} was 25.0 °C. The τ_s of Ti_3C_2 nanosheets was 334.45 s, and so the η' was calculated to be 32.7% (Figure S3).

Characteristics of Liposome. The average head group surface area per lipid molecule 'A':

$$A = A_1p_1 + A_2p_2 + A_3p_3 = 0.71\times\frac{10}{21} + 0.19\times\frac{10}{21} + 0.41\times\frac{1}{21}nm^2 = 0.45nm^2$$

The number of lipid molecules in one liposome

$$N_{tot-lip} = \frac{4\pi\times\left[R^2 + (R-T)^2\right]}{A} = \frac{4\pi\left[92^2 + (92-4)^2\right]}{0.45} = 4.53\times10^5$$

The volume of liposomes

$$V_{lip} = \frac{4\pi\times(R-T)^3}{3} = \frac{4\pi\times(92-4)^3}{3} = 2.86\times10^{-12}\mu L$$

The number of liposomes

$$N_{lip} = \frac{M_{lip} \times N_A}{N_{tot-lip}} = \frac{4.2\times10^{-5}\times6.02\times10^{23}}{4.53\times10^{5}} = 5.58\times10^{13}$$

The number of Ti_3C_2 QDs

$$N_{QDs} = \frac{m_{QDs} \times N_A}{M_{QDs}} = \frac{5\times10^{-3}\times6.02\times10^{23}}{21336} = 1.41\times10^{17}$$

The number of encapsulated Ti_3C_2 QDs per liposome

$$N_{QDs-lip} = \frac{N_{QDs} \times V_{lip}}{V_{tot}} = \frac{1.41\times10^{17}\times2.86\times10^{-12}}{1\times10^{3}} = 4.03\times10^{2}$$

where A is the average head group surface area per lipid molecule. A1, A2 and A3 were 0.71, 0.19, and 0.41 nm^2 for DPPC, cholesterol and DPPE, respectively. P1, P2 and P3 were the mole fractions of DPPC, cholesterol, and DPPE, respectively, from the molar ratio of 10:10:1:0.4. R is the hydrodynamic size from DLS measurements, T is the bilayer thickness (4.0 nm). M_{lip} is the total molar concentration of lipid including DPPC, cholesterol, and DPPE. m_{QDs} was the mass of Ti_3C_2 with a solution volume of 2.0 ml. M_{QDs} was the estimated value of the total atoms in one Ti_3C_2 QDs, assuming the QDs was a five-layered hexagonal nano flake with lateral size of 3.4 nm in consistence with the TEM image (Figure 1B).

Optimization of Experimental Conditions. To achieve an optimal analytical performance, some experimental conditions were optimized. The concentration of Ti_3C_2 QDs-encapsulated liposomes had great effect on the final temperature changing. Considering the reducing the impacts of nonspecific adsorption and increment of utilization, the different dilution ratios of Ti_3C_2 QDs-encapsulated liposomes corresponding to final temperature changing are showed in Figure S8-A. It was observed that temperature changing increased with decreasing dilution ratios of liposomes until the regent ratio was reach 1:5. When the dilution ratio was lower than 1:5, there was no obvious increase in the temperature changing. Therefore, the optimum dilution ratio of 1:5 was chosen for the subsequent assay.

Secondly, the incubation time also had great effect on the temperature change, because the biological binding for the formation of the sandwiched structure between antigen and antibody was time-consuming. As seen from Figure S8-B, the temperature increased with the increasing incubation time, and there was no significant enhancement at 30 min. For the efficient experiment, 30 min was used in this immunoassay platform.

Thirdly, the rapidly rising temperature of immunoassay platform in a few minutes was directly aroused by the irradiation of 808 nm light source and thus the irradiation time would mainly influence the temperature. It was reasonable that was an appropriate time for irradiation

when the temperature continuously increased upon irradiation until it reached a plateau. However, as shown in Figure S8-C, with the extension of irradiation time, the near infrared images of immunoassay solutions with different PSA concentration (0, 1, 2, 4, 10, and 20 ng/mL respectively) would gradually approach to the warm color. On account of the of limited color differentiation of human eye, which was sensitive to blue, green and red, we could not distinguish the image colors centralized in the scale of warm colors as clearly as that belonging to cold and warm color severally. Therefore, when the immunoassay solutions were irradiated for 180 s, the near infrared images possessed the most obvious color discrimination (from blue to red), which was optimized for rapidly semi-quantitative analysis through a portable near-infrared imaging camera.

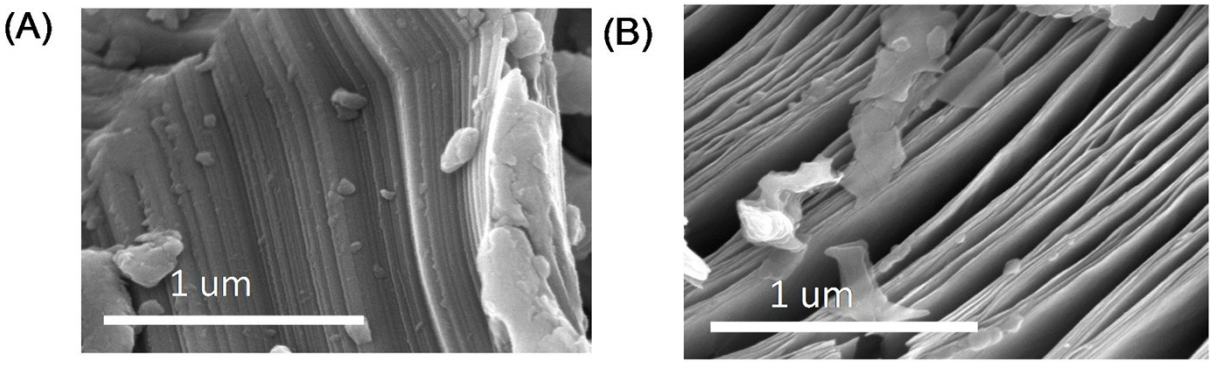

Fig. S1 Typical SEM images of (A) Ti_3AlC_2 and (B) $Ti_3C_2T_x$.

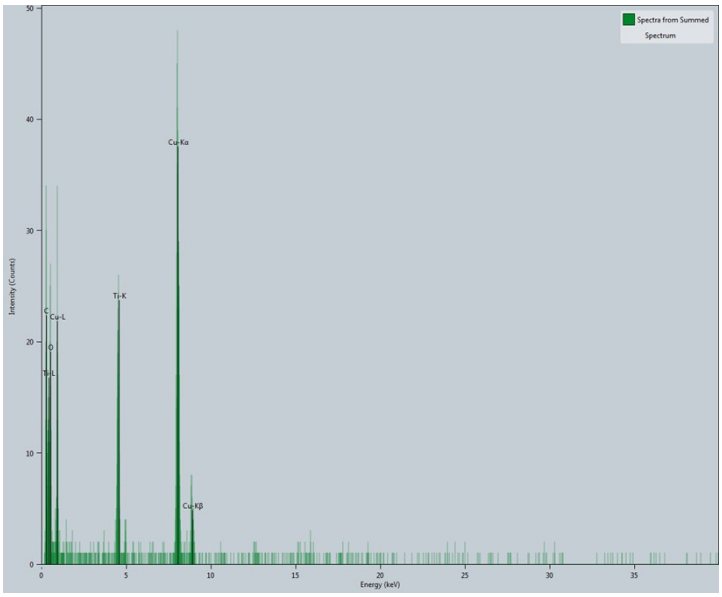

Fig. S2 Energy dispersive spectrometer of Ti_3C_2 QDs.

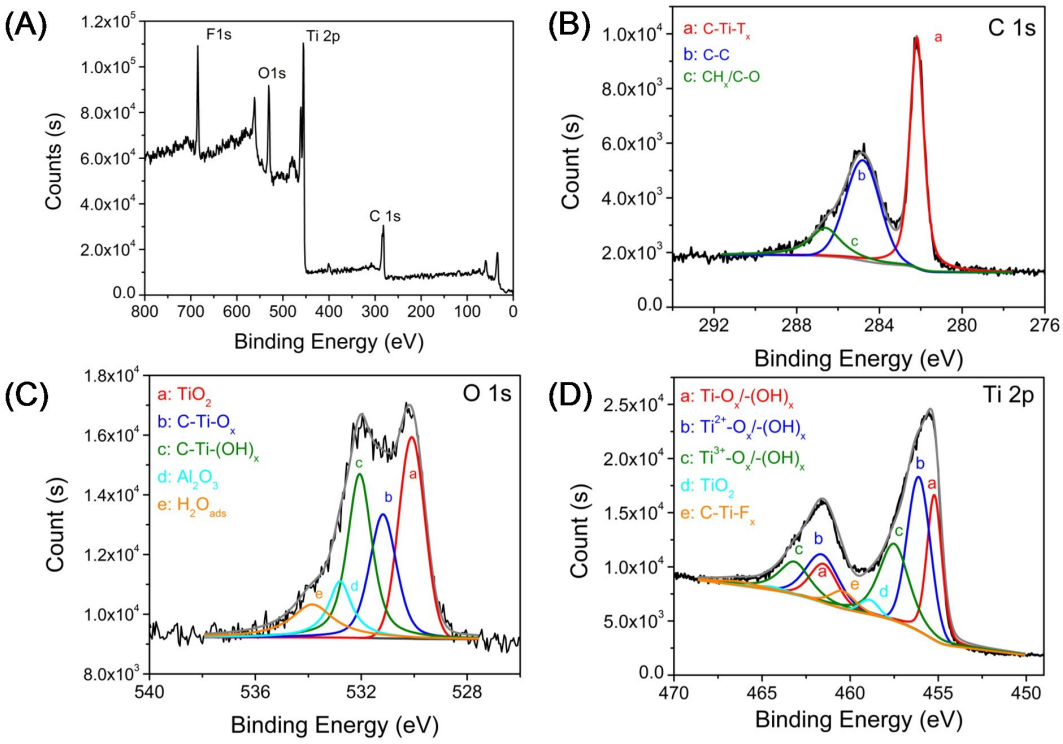

Fig. S3 (A) Survey XPS spectrum, and (B,C,D) high-resolution XPS spectra of (B) C 1s, (C) O 1s and (D) Ti 2p for $Ti_3C_2T_x$.

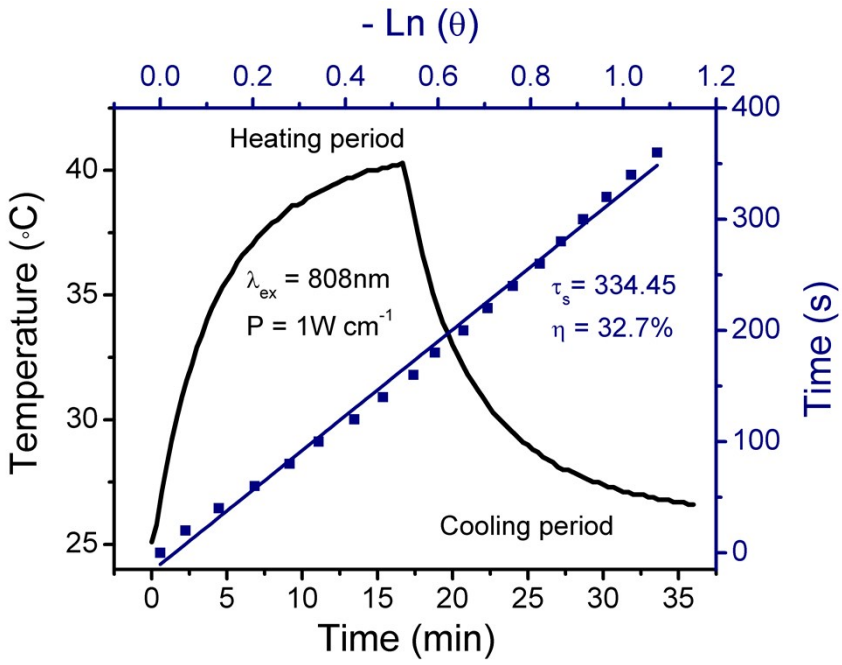

Fig. S4 Temperature profile of $Ti_3C_2T_x$ dispersed in water under irradiation with an 808-nm laser for a periods, and then the laser was turned off (black). Time constant (τs) for the heat transfer determined by the linear regression of time data from the cooling profile (blue).

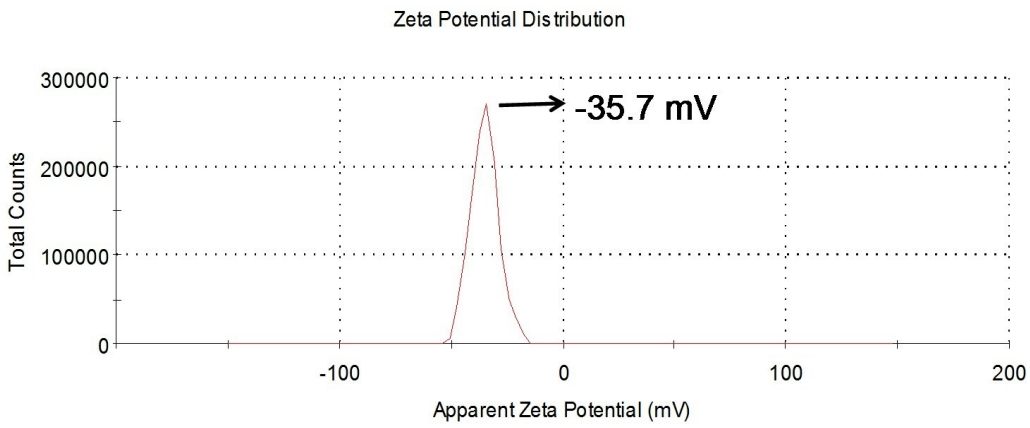

Fig. S5 ζ-Potential spectrum of Ti_3C_2 QDs dispersed in water.

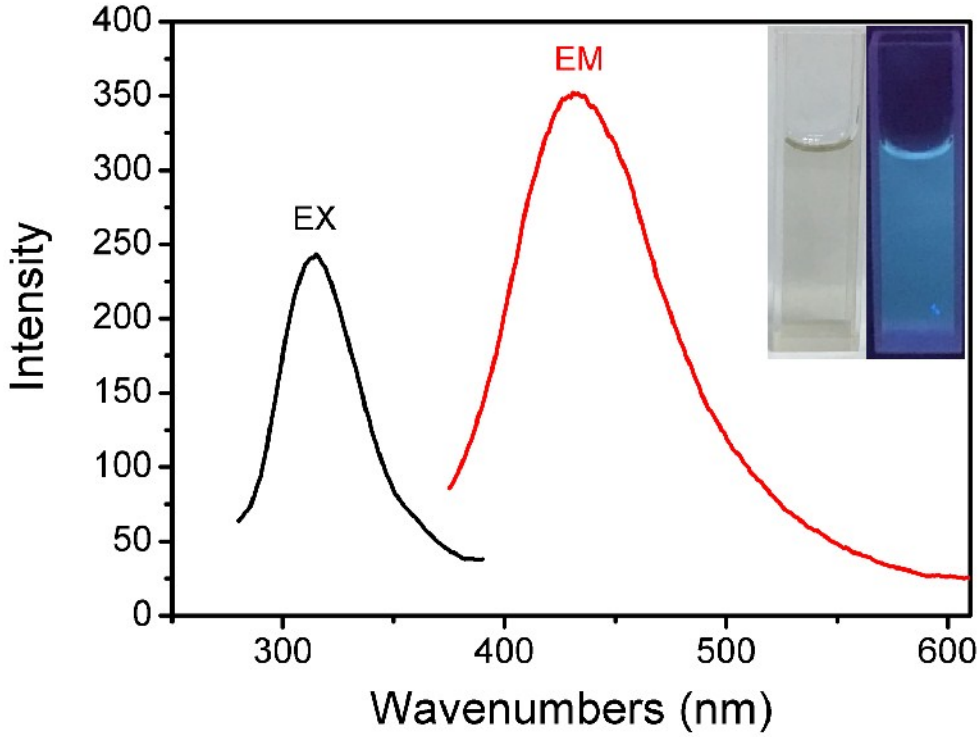

Fig. S6 PLE (λ_{em} = 425 nm) and PL (λ_{ex} = 320 nm) spectra of Ti_3C_2 QDs. Inset shows the Ti_3C_2 QDs solution under daylight (left) and 365 nm UV lamp (right).

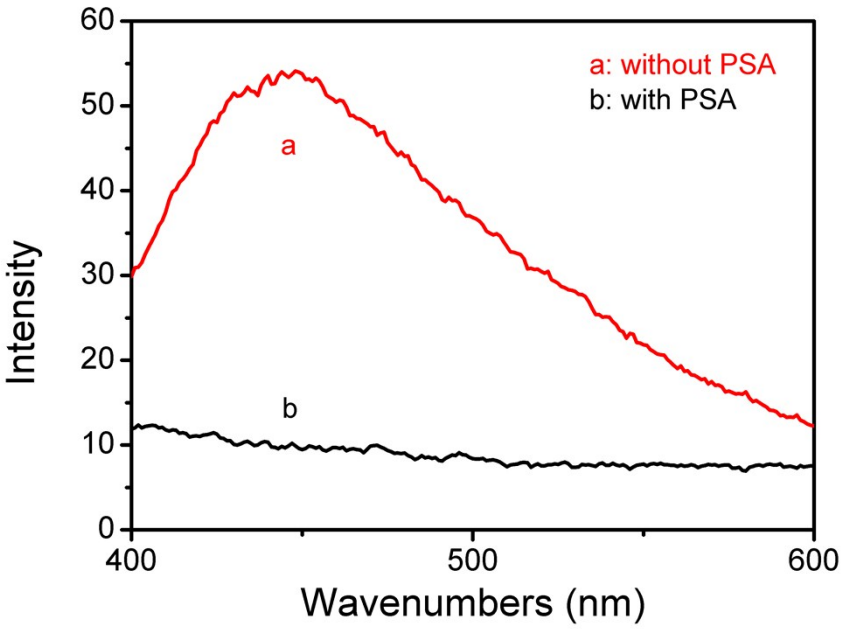

Fig. S7 PL (λ_{ex} = 320 nm) spectra of photothermal immunoassay solution in the (a) presence and (b) absence of 20 ng/mL PSA.

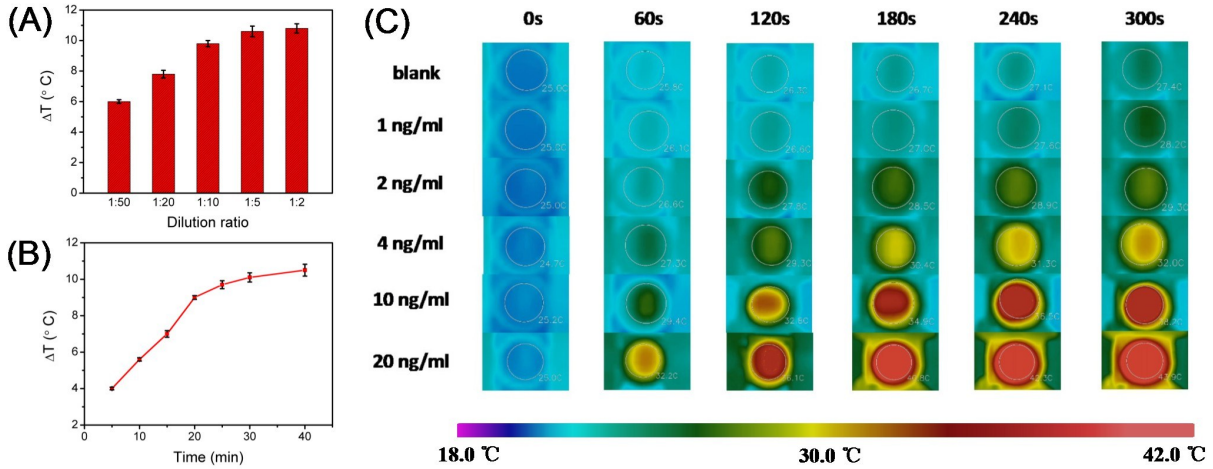

Fig. S8 Effects of (A) dilution ratio of Ti_3C_2 QDs-encapsulated liposomes conjugated with mAb2 and (B) immunoreaction time on temperature change (ΔT, $\Delta T = T_{Max} - T_{Surr}$, $T_{Surr} = T_{H2O}$) of photothermal immunoassay under irradiation of 808-nm laser for 300 sec at 1.5 W/cm^2 (PSA concentration: 10 ng/mL, used as an example). (C) Near-infrared images of the detection solution after incubation with different-concentration PSA standards (0, 1, 2, 4, 10 and 20 ng/mL) at different irradiation times (0, 60, 120, 180, 240 and 300 sec) under irradiation of 808-nm laser at 1.5W/cm^2.

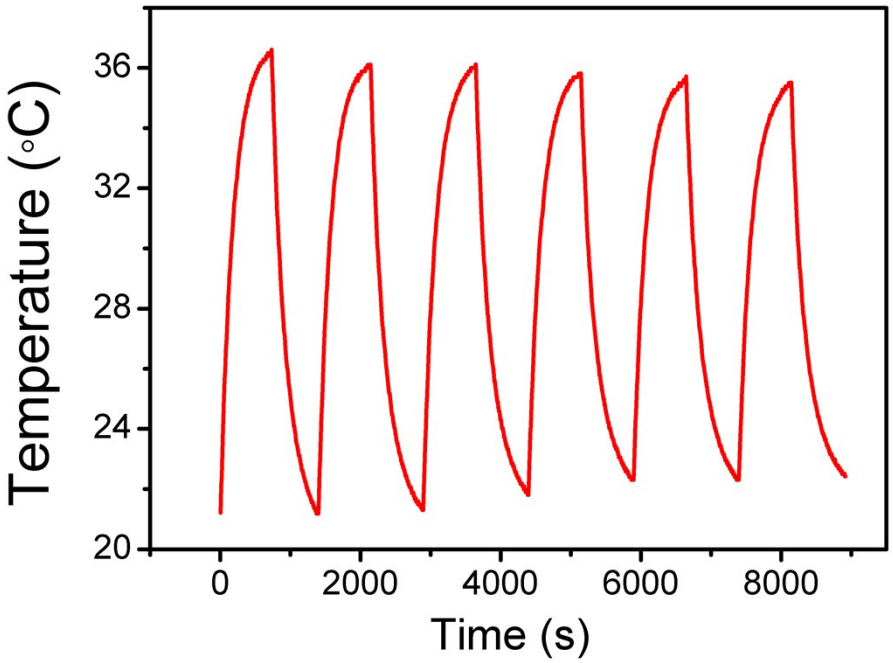

Fig. S9 Temperature responses of the detection solution containing the released Ti_3C_2 QDs on photothermal immunoassay by artificially controlling the NIR light under the 'on-off' state (10 ng/mL PSA used in this case).

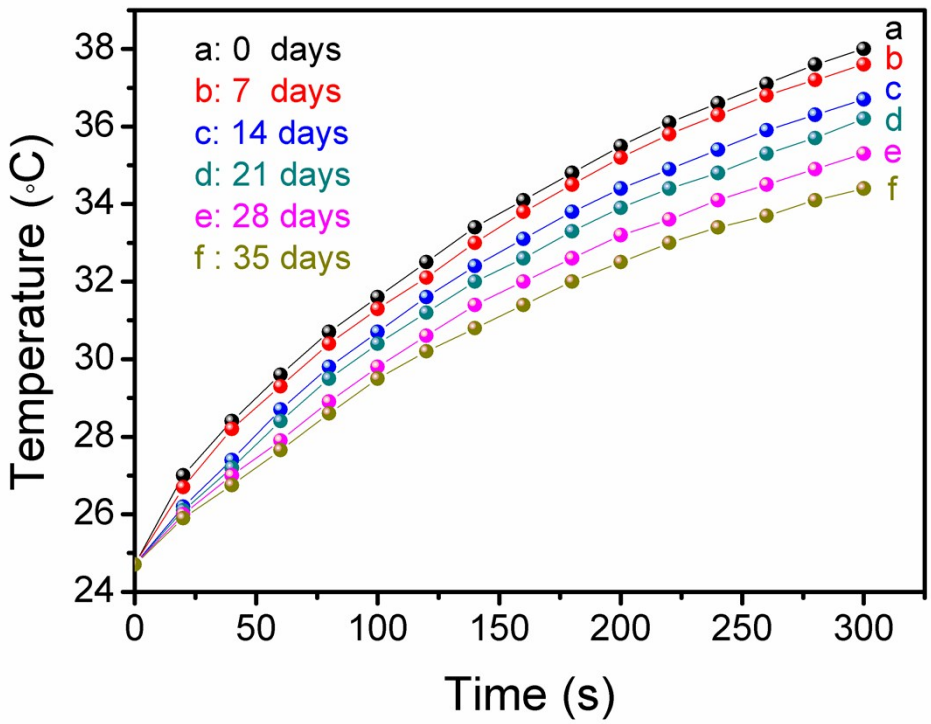

Fig. S10 Temperature responses of photothermal immunoassay by using the as-prepared Ti_3C_2 QDs-encapsulated liposomes at the differently storage days (10 ng/mL PSA used in this case).

Table S1 Comparison of the results obtained by photothermal immunoassay and human PSA ELISA kit for 8 human serum specimens containing target PSA

Matrix	Sample	Method; concentration [mean ± SD (RSD), ng/mL, n = 3]		
		photothermal immunoassay	PSA ELISA kit	t_{exp}
Human serum specimens	1	1.82 ± 0.13 (7.43%)	1.77 ± 0.11 (6.07%)	0.63
	2	34.84 ± 1.93 (5.54%)	32.39 ± 2.30 (7.10%)	1.28
	3	14.61 ± 1.21 (8.27%)	16.04 ± 1.33 (8.27%)	1.27
	4	21.01 ± 1.82 (8.71%)	19.64 ± 1.53 (7.82%)	0.99
	5	1.14 ± 0.14 (11.8%)	1.09 ± 0.06 (5.95%)	0.75
	6	4.32 ± 0.34 (7.91%)	4.09 ± 0.26 (6.38%)	0.96
	7	9.08 ± 0.68 (7.50%)	9.56 ± 0.42 (4.24%)	1.03
	8	41.27 ± 2.71 (6.59%)	43.72 ± 2.57 (5.87%)	1.10

Notes and references

1. X. Liu, B. Li, F. Fu, K. Xu, R. Zou, Q. Wang, B. Zhang, Z. Chen and J. Hu, *Dalton T.*, 2014, **43**, 11709-11715.
2. W. Ren, Y. Yan, L. Zeng, Z. Shi, A. Gong, P. Schaaf, D. Wang, J. Zhao, B. Zou and H. Yu, *Adv. Healthc. Mater.*, 2015, **4**, 1526-1536.